PERGAMON

Available online at www.sciencedirect.com

SCIENCE DIRECT®

International Journal of Heat and Mass Transfer 46 (2003) 1471–1477

International Journal of HEAT and MASS TRANSFER

www.elsevier.com/locate/ijhmt

Effect of suction/injection on the flow of a micropolar fluid past a continuously moving plate in the presence of radiation

Hassan A.M. El-Arabawy *

Mathematics Department, Faculty of Science, Ain Shams University, Cairo, Egypt

Received 7 December 1999; received in revised form 15 March 2002

Abstract

An analysis is carried out to study the effect of suction and injection on the flow and heat transfer characteristics for a continuous moving plate in a micropolar fluid in the presence of radiation. The boundary layer equations are transformed to non-linear ordinary differential equations. Numerical results are presented for the distribution of velocity, microrotation and temperature profiles within the boundary layer. The effects of varying the Prandtl number, Pr, the radiation parameter, N and porosity parameter, F_w, are determined.

1. Introduction

In recent years, the dynamics of micropolar fluids, originated from the theory of Eringen [1,2] has been a popular area of research. The equations governing the flow of a micropolar fluid involve a microrotation vector and a gyration parameter in addition to the classical velocity vector field. This theory may be applied to explain the flow of colloidal solutions, liquid crystals, fluids with additives, suspension solutions, animal blood, and many other situations.

Also, the continuous surface concept was introduced by Sakiadis [3]. Continuous surfaces are surfaces such as those of polymer sheets or filaments continuously drawn from a die.

The boundary layer flow on continuous surfaces is an important type of flow occurring in a number of technical processes. Examples may be found in continuous casting, glass fiber production, metal extrusion, hot rolling, the cooling and/or drying of paper and textiles, and wire drawing (see [4–6]). The study of heat transfer and the flow field is necessary for determining the quality of the final products of these processes as explained by Karwe and Jaluria [7,8].

Peddieson and McNitt [9] have studied the boundary layer flow of such a micropolar fluid past a semi-infinite plate, whereas a similarity solution for boundary layer flow near a stagnation point was presented by Ebert [10]. On taking into account the gyration vector normal to the xy-plane and the microinertia effects, the boundary layer flow of micropolar fluids past a semi-infinite plate was studied by Ahmadi [11]. Soundalgekar and Takhar [12] studied the flow and heat transfer past a continuously moving plate in a micropolar fluid. Perdikis and Raptis [13] studied the heat transfer of a micropolar fluid in the presence of radiation. Recently, Raptis [14] studied the flow of a micropolar fluid past a continuously moving plate in the presence of radiation.

In the present study, we have analyzed the problem of the effect of suction/injection on the flow of a micropolar fluid past a continuously moving plate in the presence of radiation.

2. Mathematical formulation

We consider a steady two-dimensional flow of a micropolar incompressible fluid past a continuously moving plate with suction or injection. The origin is located at the spot through which the plate is drawn in the fluid

* Present address: Mathematics Department, Faculty of Science 63, King Khalid University, P.O. Box 9004, Abha, Kingdom of Saudi Arabia.

0017-9310/03/$ - see front matter © 2003 Published by Elsevier Science Ltd.
PII: S0017-9310(02)00320-4

Nomenclature

C_f	friction coefficient
c_p	specific heat
E_c	Eckert number
f	dimensionless streamfunction
F_w	porosity parameter
g	dimensionless microrotation
G	microrotation parameter
G_1	microrotation constant
$h(x)$	local heat transfer coefficient
K	coupling constant parameter
k_1	mean absorption coefficient
K_1	coupling constant
N	radiation parameter
Nu_x	local Nusselt number
Pr	Prandtl number
q_r	radiative heat flux
$q_w(x)$	local heat transfer coefficient
Re_x	local Reynolds number
S	constant characteristic of the fluid
T	temperature of the fluid
T_w	temperature at the plate
T_∞	temperature of the ambient fluid
u	velocity in the x-direction
U_0	uniform velocity of the plate
U_∞	velocity in the ambient fluid
v	velocity in the y-direction
V_w	wall suction/injection velocity
x	distance along the surface
y	distance normal to the surface
Greek symbols	
η	similarity variable
κ	thermal conductivity
μ	the dynamic viscosity
ν	the kinematic viscosity
θ	dimensionless temperature function
ρ	density of the fluid
σ	microrotation component
σ_1	Stefan–Boltzmann constant

medium, the x-axis is chosen along the plate and y-axis is taken normal to it (Fig. 1).

The fluid is considered to be a gray, absorbing-emitting radiation but non-scattering medium and the Rosseland approximation is used to describe the radiative heat flux in the energy equations. The radiative heat flux in the x-direction is negligible to the flux in the y-direction.

Under the usual boundary layer approximation, the flow and heat transfer in the presence of radiation are governed by the following equations [14]

$$\frac{\partial u}{\partial x}+\frac{\partial v}{\partial y}=0, \tag{1}$$

$$u\frac{\partial u}{\partial x}+v\frac{\partial u}{\partial y}=\nu\frac{\partial^2 u}{\partial y^2}+K_1\frac{\partial \sigma}{\partial y}, \tag{2}$$

$$G_1\frac{\partial^2 \sigma}{\partial y^2}-2\sigma-\frac{\partial u}{\partial y}=0, \tag{3}$$

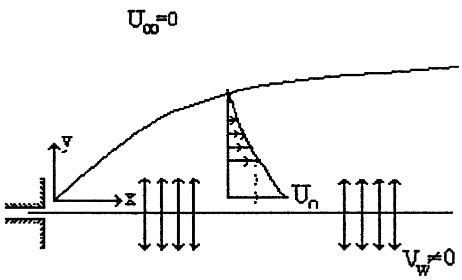

Fig. 1. Coordinate system and flow model.

$$u\frac{\partial T}{\partial x}+v\frac{\partial T}{\partial y}=\frac{\kappa}{\rho c_p}\frac{\partial^2 u}{\partial y^2}+\frac{\nu}{c_p}\left(\frac{\partial u}{\partial y}\right)^2-\frac{1}{\rho c_p}\frac{\partial q_r}{\partial y} \tag{4}$$

and the boundary conditions are given by

$$\left.\begin{array}{l} y=0: u=U_0, \quad v=V_w, \quad T=T_w, \quad \sigma=0, \\ y\to\infty: u\to 0, \quad T=T_\infty, \quad \sigma\to 0. \end{array}\right\} \tag{5}$$

Here u, v are the velocity components along x, y coordinates respectively, $\nu=(\mu+S)/\rho$ is the apparent kinematics viscosity, μ, the coefficient of dynamic viscosity, S a constant characteristic of the fluid, ρ the density, σ the microrotation component, $K_1=S/\rho(K_1>0)$ the coupling constant, $G_1(>0)$ the microrotation constant, T the temperature of the fluid, c_p the specific heat of the fluid at constant pressure, κ the thermal conductivity, q_r the radiative heat flux, U_0 the uniform velocity of the plate, V_w a non-zero velocity component at the wall, T_w the temperature of the plate and T_∞ the temperature of the fluid far away from the plate.

By using Rosseland approximation q_r takes the form

$$q_r=-\frac{4\sigma_1}{3k_1}\frac{\partial T^4}{\partial y}, \tag{6}$$

where σ_1, the Stefan–Boltzmann constant and k_1, the mean absorption coefficient.

We assume that the temperature differences within the flow are sufficiently small such that T^4 may be expressed as a linear function of temperature. This is accomplished by expanding T^4 in a Taylor series about T_∞ and neglecting higher-order terms, thus

$$T^4 \cong 4T_\infty^3 T - 3T_\infty^4. \tag{7}$$

By using (6) and (7) Eq. (4) gives

$$u\frac{\partial T}{\partial x} + v\frac{\partial T}{\partial y} = \frac{\kappa}{\rho c_p}\frac{\partial^2 u}{\partial y^2} + \frac{v}{c_p}\left(\frac{\partial u}{\partial y}\right)^2 + \frac{16\sigma_1 T_\infty^3}{3\rho c_p K_1}\frac{\partial^2 u}{\partial y^2}. \tag{8}$$

The suitable similarity variables, for the problem under consideration, are

$$\left.\begin{aligned} &\eta = y\sqrt{\tfrac{U_0}{2vx}}, \quad \psi = \sqrt{2vU_0 x f(\eta)}, \\ &\theta = \tfrac{T - T_\infty}{T_{\rm w} - T_\infty}, \quad \sigma = \sqrt{\tfrac{U_0^3}{2vx}} g(\eta), \end{aligned}\right\} \tag{9}$$

where $f(\eta)$ is the dimensionless stream function.

Defining now the velocity components as

$$\left.\begin{aligned} &u = \tfrac{\partial\psi}{\partial y} = U_0 f'(\eta), \\ &v = -\tfrac{\partial\psi}{\partial y} = -\sqrt{\tfrac{2vU_0}{x}}\left[f(\eta) - \eta f'(\eta)\right], \end{aligned}\right\} \tag{10}$$

where dashes mean differentiation with respect to η, the continuity equation is automatically satisfied and the system of Eqs. (2),(3) and (8), becomes:

$$f'''(\eta) + f(\eta)f''(\eta) + Kg'(\eta) = 0, \tag{11}$$

$$Gg''(\eta) - 2(2g(\eta) + f''(\eta)) = 0, \tag{12}$$

$$(3N + 4)\theta''(\eta) + 3NPrf(\eta)\theta'(\eta) + 3NPrE_c f''^2(\eta) = 0, \tag{13}$$

with the corresponding boundary conditions

$$\left.\begin{aligned} &f(0) = F_{\rm w}, \quad f'(0) = 1, \quad \theta(0) = 1, \quad g(0) = 0, \\ &f'(\infty) = 0, \quad \theta(\infty) = 0 \text{ and } g(\infty) = 0. \end{aligned}\right\} \tag{14}$$

In the previous equations, we have used

$K = \frac{K_1}{v}$ (Coupling constant parameter),
$G = \frac{G_1 U_0}{vx}$ (Microrotation parameter),
$N = \frac{\kappa k_1}{4\sigma_1 T_\infty^3}$ (Radiation parameter),
$Pr = \frac{\rho v c_p}{\kappa}$ (Prandtl number),
$E_c = \frac{U_0^2}{c_p(T_{\rm w} - T_\infty)}$ (Eckert number),
$F_{\rm w} = -V_{\rm w}\sqrt{\frac{2x}{vU_0}}$ (Porosity parameter).

The mass transfer parameter $F_{\rm w}$ is positive for suction and negative for injection. The shear stress at the plates is given by

$$\tau_{\rm w} = (\mu + K)\left(\frac{\partial u}{\partial y}\right)_{y=0} + K(\sigma)_{y=0}. \tag{15}$$

The friction coefficient is given by

$$C_{\rm f} = \frac{\tau_{\rm w}}{(1/2)\rho U_0^2} = -2Re_x^{-(1/2)} f''(0), \tag{16}$$

where $Re_x = U_0 x/v$ the local Reynolds number. The local heat flux may be written by Fourier's law as

$$q_{\rm w}(x) = -\kappa\left(\frac{\partial T}{\partial y}\right)_{y=0} = -\kappa(T_{\rm w} - T_\infty)\left(\frac{\rho U_0}{2\mu x}\right)^{\frac{1}{2}}\theta'(0). \tag{17}$$

The local heat transfer coefficient is given by

$$h(x) = \frac{q_{\rm w}(x)}{(T_{\rm w} - T_\infty)}. \tag{18}$$

The local Nusselt number may be written as

$$Nu_x = \frac{hx}{\kappa} = -Re_x^{1/2}\theta'(0). \tag{19}$$

3. Numerical solution

The set of non-linear ordinary differential Equations (11)–(13) with boundary conditions (14) have been solved by using the modified fourth order Runge–Kutta method along with Nachtsheim–Swigert shooting technique [15] with Pr, $F_{\rm w}$, N, K and G as prescribed parameters. The computations were done by a program which uses a symbolic and computational computer language (Mathematica 4.0) on a Pentium 1 PC machine. A step size of $\Delta\eta = 0.001$ was selected to be satisfactory for a convergence criterion of 10^{-7} in nearly all cases. The value of η_∞ was found to each iteration loop by the assignment statement $\eta_\infty = \eta_\infty + \Delta\eta$. The maximum value of η_∞, to each group of parameters Pr, $F_{\rm w}$, N, K and G, determined when the values of unknown boundary conditions at $\eta = 0$ not change to successful loop with error less than 10^{-7}.

To assess the accuracy of the present method, comparisons between the present results and previously published data [12], Table 1 below presents the comparison of $f''(0)$, also Table 2 presents the comparison of the heat transfer rates $-\theta'(0)$. In fact, this results show a close agreement, hence an encouragement for further study of the effects of other varies of parameters on the continuous moving surface.

4. Discussion of result

In many practical applications, the surface characteristics such as the local heat transfer rates are of prime

Table 1
Comparison of $f''(0)$

K	Soundalgekar and Takhar [12]	Present results
0.1	0.6291	0.622516
0.2	0.6225	0.616542

Table 2
Comparison of $-\theta'(0)$

K	G			
	Soundalgekar and Takhar [12]		Present results	
	2	4	2	4
0.1	1.944	1.946	1.93138	1.93159
0.5	1.801	–	1.93032	1.93154

Table 3
Values of $f''(0)$ and $g'(0)$ for $K = 0.2$, $G = 2$

F_w	$f''(0)$	$g'(0)$
−0.7	−0.278827	0.236917
−0.4	−0.404227	0.286997
−0.2	−0.504059	0.321165
0.0	−0.616542	0.355330
0.2	−0.741521	0.389278
0.4	−0.877517	0.422223
0.7	−1.099430	0.468923

interest. The evaluation of such quantities requires only the information contained in Tables 3–5.

The numerical results for the plate friction, plate couple stress and heat transfer rate are obtained for different values of mass transfer F_w, radiation parameter N and Prandtl number Pr.

Table 3 indicates the effect of the mass transfer F_w on the plate friction and plate couple stress. We observe that injection ($F_w \leqslant 0$) reduces the friction factor as well as plate couple stress whereas the suction has the opposite effect.

Table 4 displays the effect of the mass transfer $F_w(\geqslant 0)$, the radiation parameter N, and the Prandtl numbers Pr of the fluid on the heat transfer rate. In Table 4, we note that the heat transfer rate increases monotonically with the suction ($F_w \geqslant 0$). Also, the heat transfer rate increases monotonically with the radiation parameter N as well as Prandtl number Pr.

In Table 5, the critical values of Pr say Pr_c for which $-\theta'(0)$ attains maximum for injection ($-0.7 < F_w < 0$). It is seen that, for a given injection ($-0.7 < F_w < 0$) and radiation parameter N, the heat transfer rate increases as Pr increases until $Pr = Pr_c$ and decreases for $Pr > Pr_c$ except for ($F_w = -0.2$), the heat transfer rate increases with increases in Pr for small radiation parameter ($N = 0.1$). Moreover, for a given radiation parameter N and a Prandtl number Pr, the heat transfer rate decreases with increased injection. Therefore, the range of Prandtl numbers $[0.733, 50]$ may be represented as $[0.733, Pr_0] \cup [Pr_0, Pr_1] \cup [Pr_1, 50]$. In the first range, heat transfer rate increases with increases in radiation parameter. In the second range, the heat transfer rate has a maximum with increases in radiation parameter and in the recent range decreases with increases in radiation parameter.

Fig. 2, indicates the velocity profiles showing the effect of the mass transfer F_w. It can be seen that the ve-

Table 4
Values of $-\theta'(0)$ for various values of suction parameter with $E_c = 0.02$, $G = 2$ and $K = 0.2$

F_w	N	$Pr = 0.733$	$Pr = 7$	$Pr = 10$	$Pr = 20$	$Pr = 50$
0.0	0.1	0.148049	0.381338	0.48530	0.765469	1.31572
	5.0	0.427013	1.698650	2.06029	2.971910	4.76887
	10.0	0.460487	1.804680	2.18655	3.149290	5.04763
	∞	0.501327	1.931150	2.33700	3.360750	5.38004
0.2	0.1	0.151099	0.438375	0.567664	0.941342	1.780490
	5.0	0.492675	2.449590	3.148440	5.210750	10.61420
	10.0	0.535971	2.647820	3.408090	5.663660	11.61880
	∞	0.589180	2.891480	3.728450	6.226420	12.87760
0.4	0.1	0.154330	0.493182	0.657421	1.13350	2.296090
	5.0	0.565067	3.292290	4.381440	7.79551	17.48310
	10.0	0.618471	3.596700	4.796520	8.57451	19.34960
	∞	0.683995	3.975940	5.315350	9.55359	21.70670
0.7	0.1	0.159594	0.590839	0.804482	1.447220	3.139530
	5.0	0.686869	4.672920	6.401930	12.01480	28.52690
	10.0	0.754651	5.151590	7.071230	13.32020	31.74850
	∞	0.839313	5.753150	7.914220	14.96930	35.82610

Table 5
Values of $-\theta'(0)$ for various values of injection parameter with $E_c = 0.02$, $G = 2$ and $K = 0.2$

F_w	Pr	$N = 0.1$	$N = 5$	$N = 10$	$N = \infty$
−0.2	0.733	0.145255	0.370236	0.394953	0.422924
	1.0	0.155543	0.443520	0.472799	0.507727
	2.0	0.195481	0.646500	0.682621	0.724023
	3.0	0.219533	0.781157	0.819323	0.862524
	7.0	0.335992	1.070710	1.106100	1.144060
	10.0	0.410637	1.178190	1.207240	1.236460
	20.0	0.606922	1.300640	1.303260	1.298730
	30.0	0.738839	1.278710	1.256100	1.221140
	40.0	0.837571	1.203810	1.160150	1.101080
	50.0	0.914730	1.107830	1.047670	0.970827
	80.0	1.073920	0.805366	0.719168	0.619181
	90.0	1.111220	0.713988	0.625116	0.524610
	100.0	1.143080	0.629836	0.540432	0.441742
−0.4	0.733	0.142620	0.316706	0.334143	0.354824
	1	0.151648	0.367528	0.387032	0.409554
	2	0.179894	0.490666	0.508845	0.528099
	3.0	0.207622	0.551540	0.565012	0.577941
	7.0	0.292092	0.594600	0.587229	0.574377
	10.0	0.346541	0.557291	0.537271	0.509913
	20.0	0.469530	0.371598	0.331255	0.284557
	30.0	0.534717	0.221652	0.181967	0.140392
	40.0	0.570778	0.124587	0.093256	0.063360
	50.0	0.589723	0.066240	0.044158	0.024946
−0.7	0.733	0.138926	0.247513	0.255995	0.265478
	1.0	0.157532	0.270959	0.278802	0.286829
	2.0	0.167153	0.304162	0.304035	0.301483
	3.0	0.186060	0.293705	0.285753	0.274072
	7.0	0.234857	0.180077	0.158624	0.134169
	10.0	0.261760	0.111056	0.090657	0.069497
	20.0	0.302113	0.016252	0.009428	0.004139
	30.0	0.299892	0.000074	−0.001282	−0.002051
	40.0	0.281174	−0.002217	−0.002408	−0.002466
	50.0	0.256183	−0.002451	−0.002463	−0.002439

locity increases monotonically with injection and decreases with increases in suction.

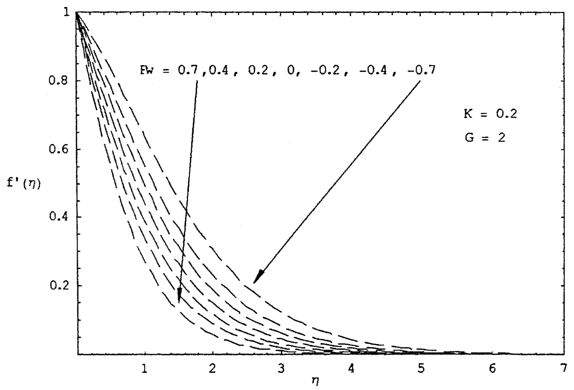

Fig. 2. Velocity profiles for various values of mass transfer.

Also Fig. 3 indicates the microrotation profiles showing effect of the mass transfer F_w. The microrotation reaches a maximum and then decay to zero.

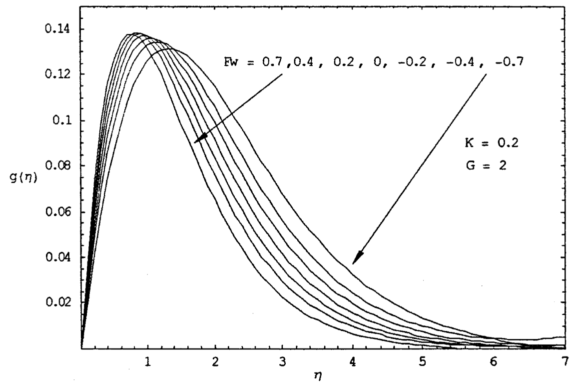

Fig. 3. Microrotation profiles for various values of mass transfer.

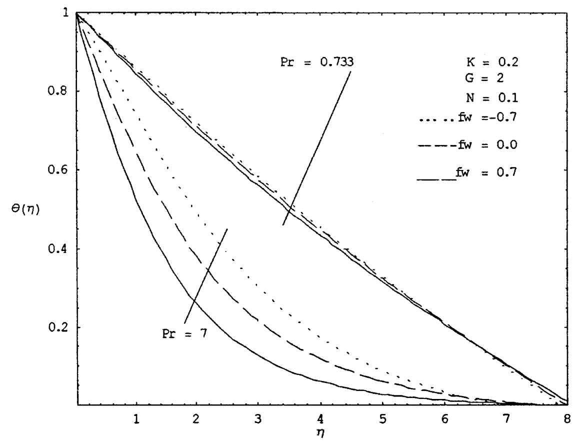

Fig. 4. Temperature profiles for various values of mass transfer.

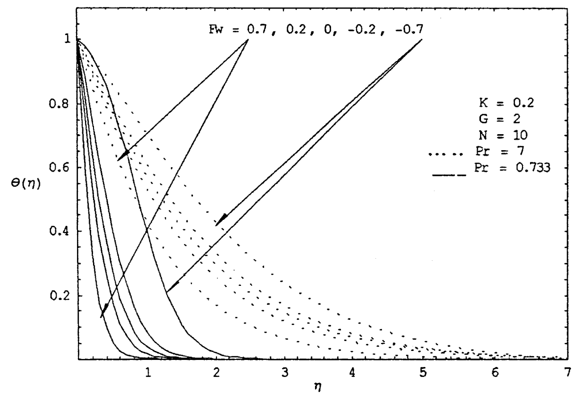

Fig. 5. Temperature profiles for various values of mass transfer.

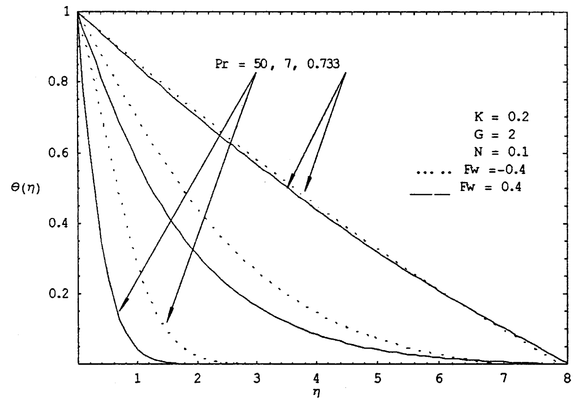

Fig. 6. Temperature profiles for various values of Pr and mass transfer.

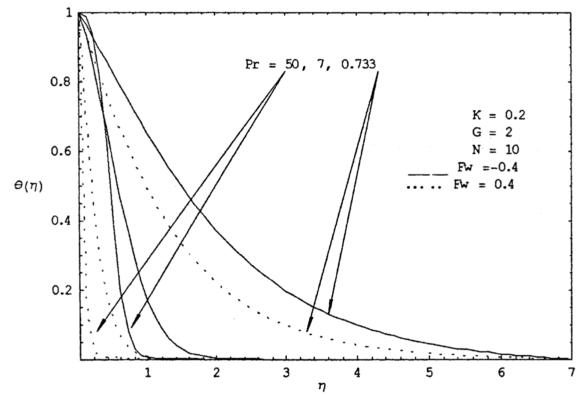

Fig. 7. Temperature profiles for various values of Pr and mass transfer.

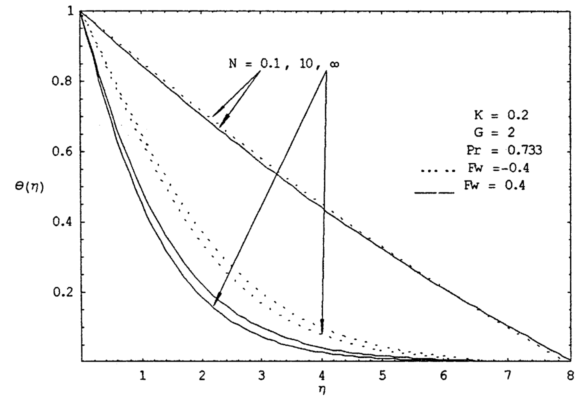

Fig. 8. Temperature profiles for various values of radiation parameter and mass transfer.

Increasing values of the injection parameter move the location of the maximum value of the microrotation away from the surface. The locations of the maximum value of the microrotation profiles as a whole are less with increases in suction.

Figs. 4–9 show the temperature profiles for various values of mass transfer F_w, radiation parameter N, and Prandtl numbers Pr of the fluid. Figs. 4 and 5 show the effect of F_w on the temperature profile for different Prandtl numbers at a fixed value of N. It can be seen from Figs. 4 and 5 that the temperature profile at any point in the fluid decreases with suction and increases with injection. For small N, this effect is reversed after a point of accumulation with $Pr = 0.733$.

Figs. 6 and 7 show the effect of Prandtl number on the temperature profile for different mass transfer F_w at a fixed value of N. It can be seen from Figs. 6 and 7 that the temperature profile at any point in the fluid decreases with Pr.

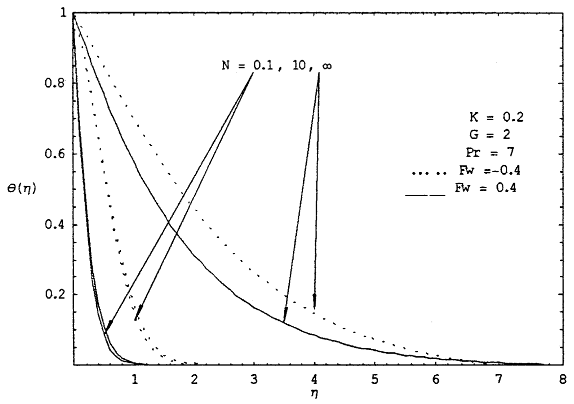

Fig. 9. Temperature profiles for various values of radiation parameter and mass transfer.

Figs. 7 and 8 show the effect of radiation parameter on the temperature profile for different mass transfer F_w at a fixed value of *Pr*. It can be seen from Figs. 7 and 8 that the temperature profile at any point in the fluid decreases with N.

5. Conclusions

In this paper we have extended the problem of the flow of a micropolar fluid past a continuously moving plate by the presence of radiation which was studied by Raptis [14] to include the effects of suction and injection. The presence of suction and injection serves to introduce one extra parameter into the problem, namely F_w. The effects of the mass transfer, F_w, the fluid Prandtl number, *Pr*, and the radiation parameter, N on the heat transfer rate and the flow and temperature profiles are examined. In general, the heat transfer rate increases monotonically with suction ($F_w \geqslant 0$), the radiation parameter and the Prandtl number. For the case of injection ($F_w < 0$), the heat transfer rate was reported to decrease with increased injection. The heat transfer rate was also found to oscillate and be dependent on a critical Prandtl number and radiation parameter.

References

[1] A.C. Eringen, Int. J. Eng. Sci. 2 (1964) 205.
[2] A.C. Eringen, Theory of micropolar fluids, J. Math. Mech. 16 (1966) 1–18.
[3] B.C. Sakiadis, Boundary layer behavior on continuous solid surface; the boundary layer on a continuous flat surface, Am. ICHE J. 7 (1961) 221.
[4] T. Altan, S. Oh, H. Gegel, Metal Forming Fundamentals and Applications, American Society of Metals, Metals Park, OH, 1979.
[5] E.G. Fisher, Extrusion of Plastics, Wiley, New York, 1976.
[6] Z. Tadmor, I. Klein, Engineering principles of plasticating extrusion, Polymer Science and Van nostrand Reinhold, Van nostrand Reinhold, New York, 1970.
[7] M.V. Karwe, Y. Jaluria, Fluid flow and mixed convection transport from a moving plate in rolling and extruasion processes, J. Heat Transfer 110 (1988) 655–661.
[8] M.V. Karwe, Y. Jaluria, Numerical simulation of thermal transport associated with a moving flat sheet in materials processes, J. Heat Transfer 113 (1988) 655–661.
[9] J. Peddieson, R.P. McNitt, Boundary layer theory for micropolar fluid, Recent Adv. Eng. Sci. 5 (1970) 405–426.
[10] F. Ebert, Chem. Eng. J. 5 (1973) 85.
[11] G. Ahmadi, Self-similar solution of incompressible micropolar boundary layer flow over a semi-infinite plate, Int. J. Eng. Sci. 14 (1976) 639.
[12] V.M. Soundalgekar, H.S. Takhar, Flow of a micropolar fluid on a continuous moving plate, Int. J. Eng. Sci. 21 (1983) 961.
[13] C. Perdikis, A. Raptis, Heat transfer of a micropolar fluid by the presence of radiation, Heat Mass Transfer 31 (1996) 381–382.
[14] A. Raptis, Flow of a micropolar fluid past a continuously moving plate by the presence of radiation, Int. J. Heat Mass Transfer 41 (1998) 2865–2866.
[15] J.A. Adams, D.F. Rogers, Computer-Aided Heat Transfer Analysis, McGraw-Hill, 1973.